Hindawi
Geofluids
Volume 2022, Article ID 9889714, 12 pages
https://doi.org/10.1155/2022/9889714

Research Article

Ranking and Evaluation of Tight Sandstone Reservoirs and the Determination of the Lower Limit of Reservoir Physical Properties: A Case Study of Longfengshan Area in the Southern Songliao Basin, China

Weiming Wang,[1] Yingnan Liu,[1] Changsheng Miao,[2] Yuhu Liu,[3] Xiyu Qu,[1] Yangchen Zhang,[1] Weihao La,[1] and Qixia Lv[1]

[1]*School of Earth Science and Technology, China University of Petroleum (East China), Qingdao, 266580 Shandong, China*
[2]*School of Exploration and Mapping Engineering, Changchun Institute of Technology, Changchun, 130062 Jilin, China*
[3]*PetroChina North China Petrochemical Company, Changchun, 130062 Jilin, China*

Correspondence should be addressed to Yingnan Liu; 229228506@qq.com

Received 22 March 2022; Revised 29 April 2022; Accepted 6 May 2022; Published 25 May 2022

Academic Editor: Dengke Liu

Ranking, evaluation, and the determination of the lower limit of physical properties (PPLL) are critical for selecting the sweet spots of tight reservoirs. This study investigated the tight reservoirs in the Longfengshan area in the southern Songliao Basin. Based on reservoir evaluation, this study determined the ranking criteria and the PPLL of tight sandstone reservoirs. The results are as follows. (1) Tight sandstone reservoirs can be divided into I, II, and III types based on the energy storage parameter and pore structure. Reservoirs with a porosity of > 6% are I-type reservoirs. The reservoirs of this type have high accumulation and seepage capacities, and their pore structures feature low displacement pressure and high structure coefficients. Reservoirs with a porosity of < 4% are III-type reservoirs. The reservoirs of this type have low accumulation and seepage capacities, and their pore structures feature high displacement pressure and low structure coefficients. The remaining reservoirs are II-type reservoirs. (2) The PPLL (denoted by porosity) of tight sandstone reservoirs was determined to be 2.50% using the water film thickness method and the minimum pore throat radius method. The water film thickness method, which comprehensively considers the geological factors including formation temperature, formation pressure, and the adsorption capacity of minerals, is innovative to a certain degree. As verified by the test data from the major exploration wells drilled in the Longfengshan area, the ranking criteria of tight reservoirs proposed in this study are effective and highly applicable and thus serve as effective guidance on the future exploration of the study area.

1. Introduction

Tight sandstone oil and gas reservoirs enjoy high permeability and can be stimulated by fracturing. Therefore, they are greatly practical in increasing the reserves and production of unconventional oil and gas in China [1–3]. Currently, the exploration and development of tight sandstone oil and gas resources in China are in the golden period of rapid development after experiencing theoretical and technical preparation and promotion of national policies [4–6]. Although breakthroughs in tight sandstone gas have been made in the Ordos, Songliao, Junggar, and Sichuan basins, the gas reservoirs in these basins are generally deeply buried and have complex diagenesis, low component maturity, high content of rock debris, and grain contacts dominated by line, convex-concave, or sutured contact [7, 8]. These features pose difficulties to the geological evaluation of shale gas sweet spots of tight reservoirs. Therefore, there is an urgent need to carry out the ranking and evaluation of tight reservoirs and to determine the PPLL of the reservoirs.

As the research deepens, various methods for ranking and evaluating reservoirs are constantly emerging [9]. Among them, traditional methods use the relationships of porosity and permeability with the productivity of reservoirs based on the understanding of the lithological and lithofacies characteristics of reservoirs [10–12]. Common methods are as follows: (1) Method of classifying reservoirs according to the types and structures of pores on rock surfaces. This type of method comprehensively evaluates the storage capacity of reservoirs based on casting thin sections, large number of observations using scanning electron microscopes, and the lithological and lithofacies characteristics of rocks. (2) Method of classifying reservoirs according to the characteristics of the capillary pressure curves of sandstones. This type of method ranks reservoirs in the order of sensitive parameters such as displacement pressure and median pore throat radius selected primarily based on capillary pressure curves. (3) Method of simply classifying reservoirs according to their physical properties. This method can roughly reflect the quality and distribution of reservoirs based on a large amount of porosity and permeability data. Massive studies have been conducted on the determination of the PPLL of reservoirs using the methods such as empirical statistics, well test, induction according to oil-bearing occurrence, mercury injection parameter, and irreducible water saturation [13, 14]. These methods for ranking reservoirs and determining the PPLL work for conventional reservoirs with favorable pore structures and abundant data of well tests. Moreover, their evaluation accuracy and reliability depend entirely on the number of samples, and they usually fail to predict and guide tight reservoirs. Given this, this study investigated the tight sandstone reservoirs in the deep strata of the Longfengshan area in the southern Songliao Basin. Given the high clay content and small pore throats of the reservoirs, this study determined the ranking boundaries and PPLL of the reservoirs based on the microscopic pore structure and oil and gas enrichment of the reservoirs using the energy storage parameter, pore structure parameters, water film thickness, and the minimum pore throat radius that allows fluids to flow (also referred to as the minimum flow pore throat radius).

2. Background of the Study Area and Tests

2.1. Background of the Study Area. The Changling fault depression is located in the central depression area of the southern Songliao Basin. It is a Late Mesozoic volcanic and clastic basin developing on Mesozoic metamorphic basement and has superposed faults and depressions. With the faulted strata covering an area of 7240 km^2, the Changling fault depression is one of the largest sags in the Songliao Basin. Moreover, the basement of the Changling fault depression has a maximum burial depth of over 8000 m. The Changling fault depression connects the Gulong fault depression in the north and is adjacent to the Shuangliao fault depression in the south. Meanwhile, the Da'an, Haituo, and Tongyu fault depressions lie on its west side, and the Gudian and Fulongquan fault depressions lie on its east side (Figure 1).

The Longfengshan area lies in the southern part of the Changling fault depression, covering an area of about 300 km^2. Strata in this area include the Shahezi, Yingcheng, Denglouku, Quantou, Qingshankou, Yaojia, and Nenjiang formations from bottom to top. In the early deposition period of the Shahezi Formation, the sedimentary facies in the Longfengshan sub-sag include fan deltas, sublacustrine fans, and semi-deep to deep lacustrine facies. In the late deposition period of the Shahezi Formation, the Longfengshan area experienced continuous and rapid expansion, the lake level rose, and the lacustrine basin expanded. In contrast, the fan delta sedimentary system shrank and was gradually transformed into a sublacustrine-fan sedimentary system dominated by gravity-flow deposits. In the early deposition period of the Yingcheng Formation, the sedimentary facies in the Longfengshan sub-sag include fan deltas, shore-shallow lacustrine facies, and semi-deep to deep lacustrine facies. In this period, the fan deltas in the southern part of the Changling sub-sag were smaller than in the deposition period of the Shahezi Formation. In the middle-late deposition period of the Yingcheng Formation, the sedimentary area in the Longfengshan area gradually expanded, so did the sedimentary area of the Fan delta. Meanwhile, glutenite masses in the area experienced gradual progradation toward the deep part of the lacustrine basin [15–17]. In 2014, a breakthrough was made in the tight sandstone natural gas in the Yingcheng Formation, and its major gas zones III, IV, V, and VI were successively discovered. It is expected that this formation has geological reserves of 234.43×10^8 m^3 and technically recoverable reserves of 105.45×10^8 m^3. Drilling has revealed that the Longfengshan area has great potential for tight sandstone gas resources [18, 19].

2.2. Experiments and Tests. To obtain detailed pore throat structures of tight sandstone reservoirs and key parameters used in ranking and evaluating the reservoirs and determining the PPLL of the reservoirs, this study designed multiple experiments and tests of porosity, permeability, wetting angle, mercury injection capillary pressure (MICP), nuclear magnetic resonance (NMR), and low-temperature nitrogen adsorption ([20–23], [24, 25]). Different core samples are required for different experiments and tests. Given the heterogeneity of reservoirs in the study area, the test plan was optimized in this study. This plan tried to ensure that the experiments and tests of porosity, NMR, and MICP were conducted using samples from the same columnar core based on the characteristics of various experiments and tests. In this way, fewer rock samples were required and, importantly, the impact of reservoir heterogeneity can be reduced, thus ensuring that the tests were comparable. The optimized test process is as follows. (1) Wash the samples to remove oil and then dry the samples; (2) prepare standard columnar cores each with a size of 2.5 cm ×2.5 cm, and then cut about 3–5 g of crushed samples from two core sections for low-temperature nitrogen adsorption experiments; (3) determine the porosity and permeability of standard columnar cores; (4) conduct NMR experiments; (5) cut samples used in NMR experiment into two sections, one of which was used for the wetting angle experiment and the other for the MICP experiments.

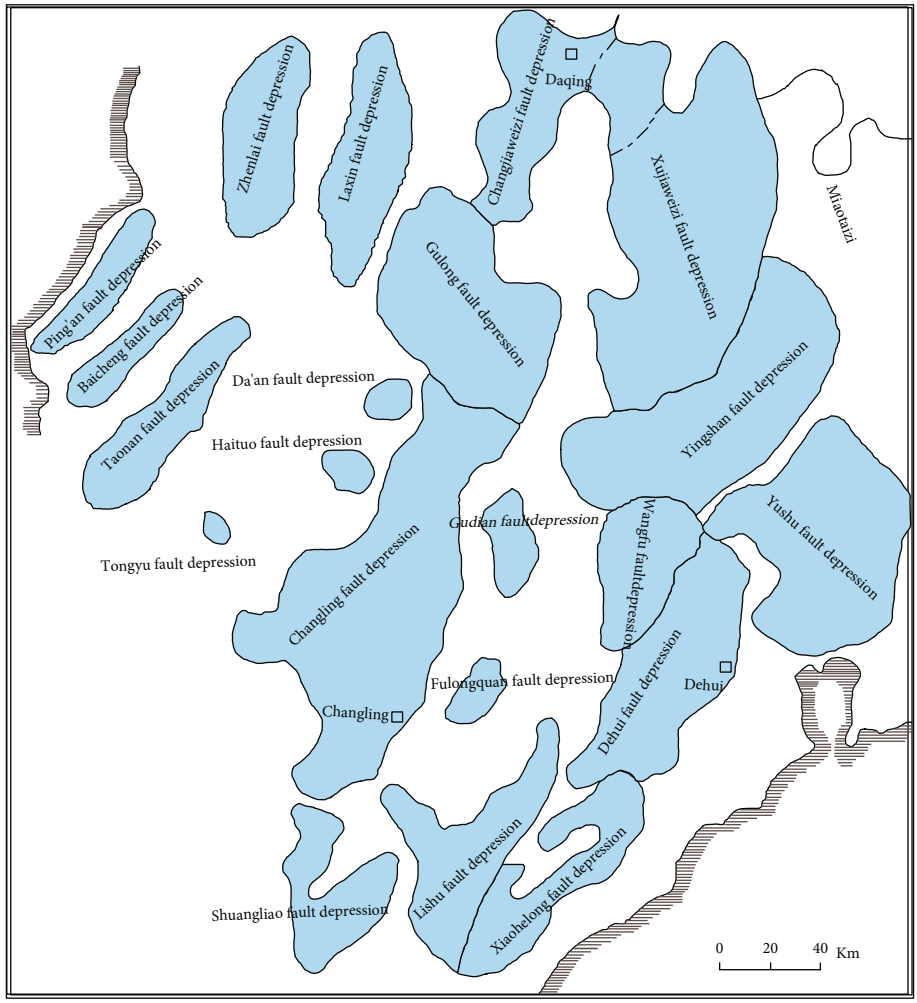

Figure 1: Map showing the distribution of main fault depressions in the southern Songliao Basin [19].

The porosity and permeability of rocks were measured as per SY/T 5336-1996 *Method of Core Routine Analysis*, a Chinese oil and gas industry standard. Given that more small pores should be discovered in the tight reservoirs in the study area, the helium injection method was employed. The basic process of this method is as follows. (1) Under certain pressure, expand a specific volume of helium to the core chamber under atmospheric pressure until an equilibrium state is reached. (2) Measure the pressure and calculate the sum of the volume of injected helium and the volume of the core chamber. (3) Determine the pore volume of the rock sample by connecting the core holder to the helium porosimeter. The air permeability of rocks was tested by making dry gas pass through the core and then measuring the pressure difference and flow rate. The MICP experiments were conducted using an AutoPore IV 9505 porosimeter. In this experiment, liquid mercury was injected into the treated sample. A certain volume of mercury entered the pores of rocks subject to the pressure difference before and after mercury injection. Afterward, the mercury injection and withdrawal curves could be plotted based on the changes in pressure and the volume of injected mercury. Then, other characteristic parameters of pore structure can be further calculated. Compared with conventional mercury injection methods, high-pressure mercury injection had a maximum mercury injection pressure of 200 MPa, corresponding to the minimum pore throat radius of 3.68 nm, and thus can effectively reflect the characteristics of micro/nanopores of tight reservoirs. This experiment was carried out under an environmental temperature of 21.3°C–21.5°C and relative humidity (RH) of 40%–44%. The low-temperature nitrogen adsorption experiments were carried out using BSD-PS-series automatic specific surface area and porosity analyzer and the steps are as follows. First, the samples were degassed at a high temperature of 150°C for three hours. Then, the isotherm adsorption-desorption curves of the samples were obtained by static volume method at an absolute temperature of 77 K. The detection range of pore size was 0.4–200 nm in the experiment. The NMR experiments were performed using a MicroMR23-060V NMR analyzer, and the process is as follows. (1) The NMR signals of the core sample saturated with water were calibrated by referring to the samples with standard scales, and the signal intensity was converted into porosity. Attenuated echo signals were obtained during the collection of the water-saturated sample. Then, the NMR T2 spectrum

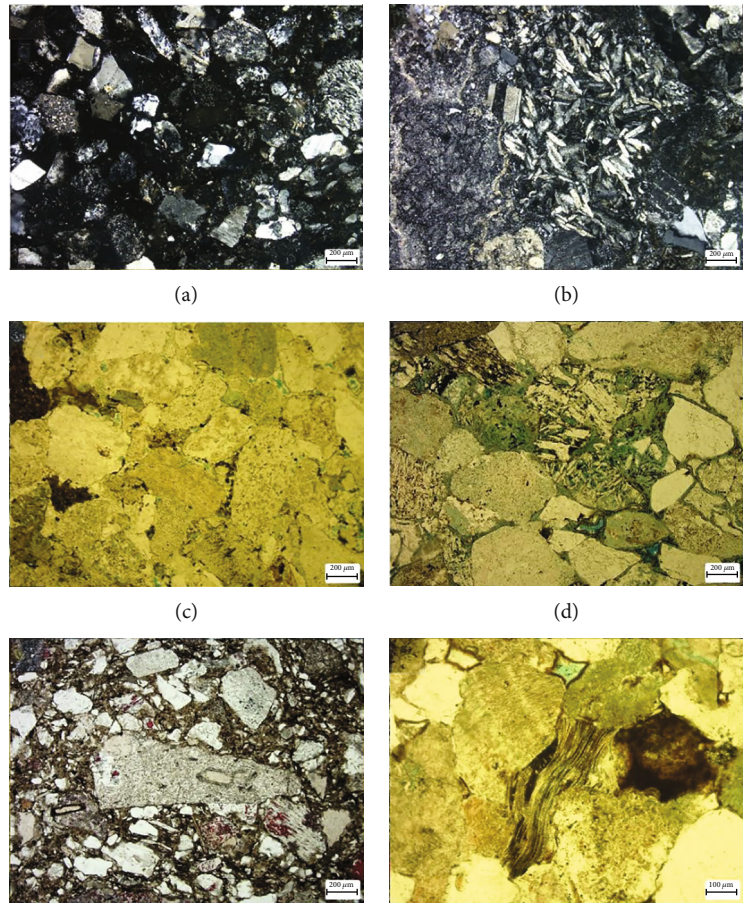

Figure 2: Petrological characteristics of tight clastic reservoirs. (a) Well Bei210, -4127.7 m, feldspathic litharenites, cross-polarized light; (b) Well Bei210, -4129.65 m, litharenites, cross-polarized light; (c) Well Bei203, -3317.87 m, litharenites, plane-polarized light; (d) Well Bei202, -3112.75 m, litharenites, plane-polarized light; (e) Well Bei203, -3615.5, matrix support, plane-polarized light; (f) Well Bei201, -3398.01 m, grain support, plane-polarized light.

of the sample was acquired through mathematical inversion of the attenuated echo signals using the SIRT inversion algorithm. Afterward, the NMR T2 cutoff was obtained using the porosity accumulation curves of water-saturated samples and centrifuged samples. Then, the saturation of both irreducible and movable fluids was calculated. The wetting angle was measured using a contact angle goniometer LT/Y 2009-005. The QB/T pendant drop method was used to observe the shapes and size of droplets, and the RealDrop contour analysis method was used to automatically generate drop samples and analyze the surface tension and various geometric sizes of droplets.

3. Results

3.1. Basic Characteristics of the Tight Sandstone Reservoirs. In terms of lithological characteristics, the rocks in the tight sandstone reservoirs mainly include medium-fine- and coarse-grained sandstones, which contain gravels mostly. They have a low matrix content (generally less than 5%) and widely ranging cement content (average: 17.35%). Clastic grains in the reservoirs are dominated by rock debris, followed by quartz and feldspar. Their components have a low maturity. Since the reservoirs are a set of near-source deposits, their clastic grains show poor sorting, the coexistence of grain support to matrix support, and sub-angular to subcircular shapes mostly. Moreover, they have complex grain contacts, with point contacts, line contacts, and convex-concave contacts all visible. The most common cementation types include film-pore, continuous crystal, and crystal mosaic types (Figure 2).

The tight clastic reservoirs in the study area have poor physical properties. The tight reservoirs in the Yingcheng Formation have an average porosity of 4.16% and an average permeability of 0.68 mD, with the porosity mainly concentrated in 2%–6% and the permeability dominated by 0.1–0.5 mD. Compared with the reservoirs in the Yingcheng Formation, the tight sandstone reservoirs in the Shahezi Formation generally have lower physical properties. Specifically, their porosity is mostly less than 2% and is only 2.13% on average. Their permeability is close to that of the Yingcheng Formation. It is concentrated in 0.1–0.5 mD, with an average of 0.283 mD.

In terms of pore structure, all the MICP curves of the study area show the characteristics of negative skewness of slanting degree, reflecting poor pore structure. Figure 3

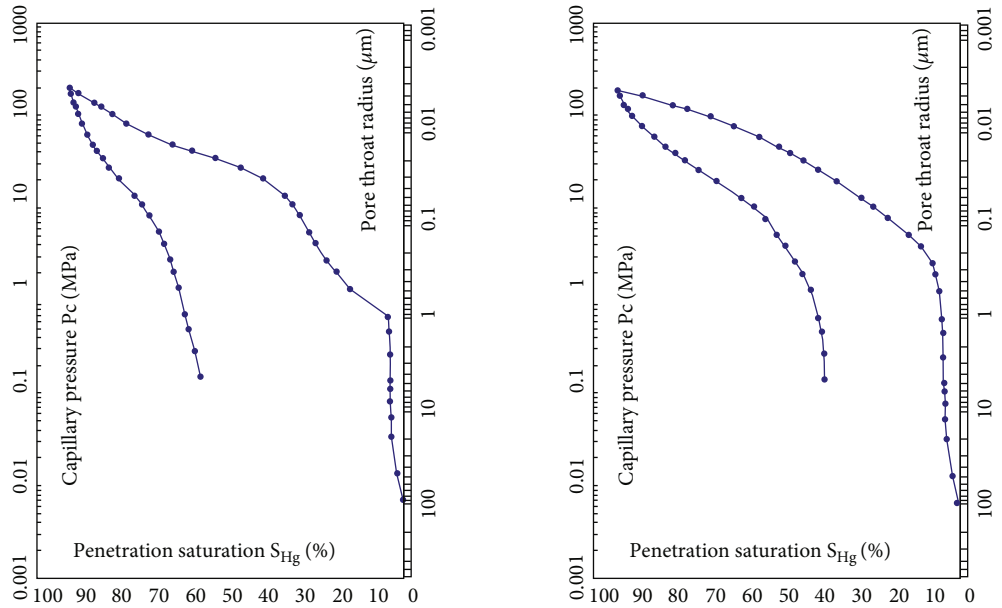

(a) Well Bei204 in the Yingcheng Formation, depth: 2368.78 m (b) Well Bei208 in the Shahezi Formation, depth: 3590.12 m

Figure 3: Capillary pressure curves of faulted strata in the Longfengshan area ((a) Yingcheng Formation; (b) Shahezi Formation).

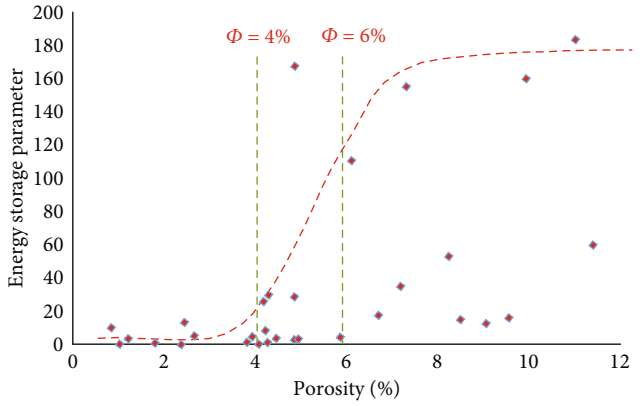

Figure 4: Relationship between porosity and the energy storage parameter.

shows the capillary pressure curves of representative samples from the Yingcheng and Shahezi formations. According to this figure, the curves lack a smooth section in their middle parts, further indicating that the reservoirs have widely varying pore size, high displacement pressure, and poor sorting.

Based on the above analyses of lithology, physical properties, and pore structures, the reservoirs in the study area are characterized by poor physical properties, complex pore structures, greatly different pore throat sizes, and poor connectivity.

3.2. Ranking of the Tight Sandstone Reservoirs. It is necessary to fully consider the pore structure in ranking and evaluating tight reservoirs in the Longfengshan area. The key to the effective evaluation and development of tight gas reservoirs is to select preferred disposable tight reservoirs [26, 27].

(1) Energy storage parameter

Unlike conventional reservoirs, tight reservoirs show a poor correlation between porosity and permeability. In other words, reservoirs with a high porosity may have a very low permeability due to their complex pore structure. The heterogeneity of the porosity and permeability affects the accumulation of natural gas. However, a complex pore structure is conducive to the preservation of natural gas [28]. This study selected the three most common parameters for reservoir evaluation, namely, porosity, permeability, and gas saturation. As the porosity increases, natural gas is more liable to accumulate in reservoirs and the gas saturation correspondingly increases. Meanwhile, a high permeability suggests high natural gas mobility in tight reservoirs. To comprehensively consider the impacts of the porosity and permeability of tight reservoirs on the enrichment of tight gas, the continued product of the three parameters was considered the new energy storage parameter to comprehensively reflect the availability of tight gas reservoirs. The equation is:

$$A = \varphi \times K \times Sg, \tag{1}$$

where

A - energy storage parameter, $\times 10^{-7}\,\mu m^2$

φ - porosity, %

K - permeability, $\times 10^{-3}\,\mu m^2$

Sg - gas saturation, %.

The constructed energy storage parameter can be easily acquired and has clear geological significance. According to Equation (1), a higher energy storage parameter value suggests a higher enrichment level and higher tight gas mobility, and vice versa.

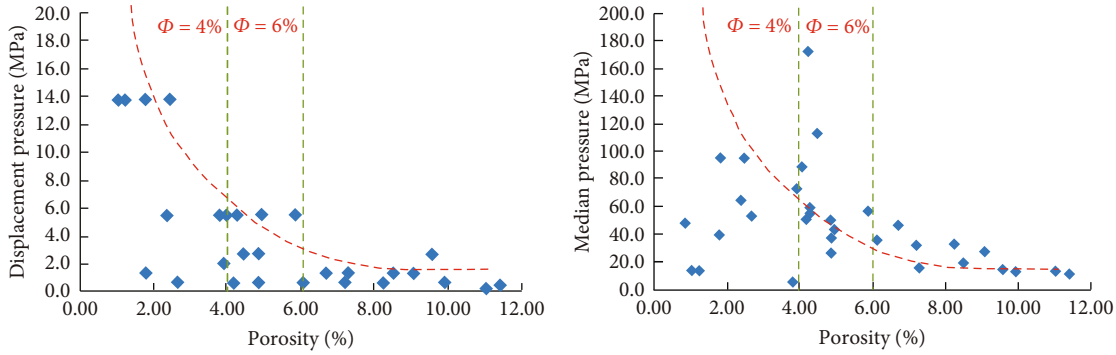

(a) Relationships of displacement pressure with porosity (b) Relationships of median pressure with porosity

Figure 5: Relationships of displacement pressure and median pressure with porosity. ((a) Relationships of displacement pressure with porosity. (b) Relationships of median pressure with porosity.).

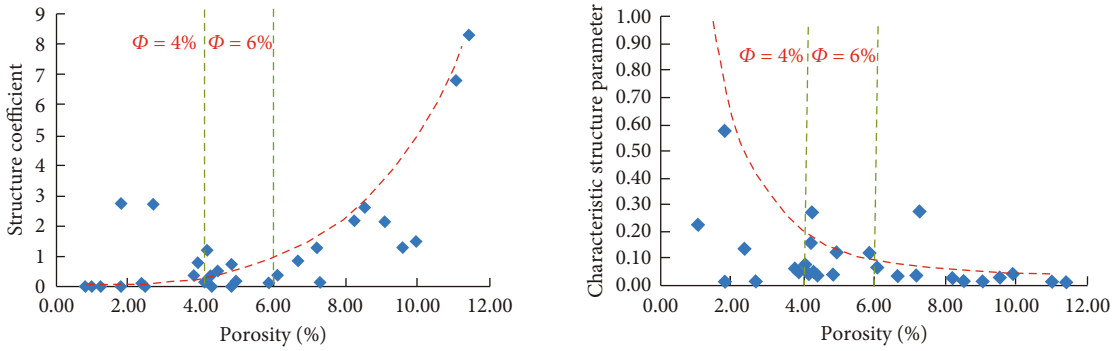

(a) Relationships of the structure coefficient with porosity (b) Relationships of the characteristic structure parameter with porosity

Figure 6: Relationships of the structure coefficient and the characteristic structure parameter with porosity. ((a) Relationships of the structure coefficient with porosity. (b) Relationships of the characteristic structure parameter with porosity.).

(2) Determining ranking boundaries using the relationship between energy storage parameter and porosity

The energy storage parameter can relatively reflect the enrichment and tight gas mobility in terms of composition. However, a single parameter cannot reflect the ranking boundaries of reservoirs. Therefore, this study used the relationship between the energy storage parameter and the porosity to make the reservoir ranking boundaries correspond to the porosity—the more commonly used parameter. This study established the relationship between the energy storage parameter and the porosity rather than the relationship between the energy storage parameter and the permeability for the following reasons. (1) Compared to porosity, the permeability of tight reservoirs suffers high analytical errors and is less practical. (2) In terms of microscopic pore characteristics of reservoirs, the regular changes in the porosity of tight reservoirs reflect the changes in pore size and specific surface area besides the reservoir space [29].

Figure 4 shows the relationship between the energy storage parameter and the porosity in the Longfengshan area in the Songliao Basin. According to this figure, the energy storage parameter can be divided into three areas, namely, low-value, rising, and high-value areas. In the area with a porosity of < 4%, the energy storage parameter is very low, indicating small storage space and low gas saturation of tight reservoirs. Moreover, the tight gas in this area has low mobility due to poor physical properties. In the area with a porosity of 4%–6%, the energy storage parameter rises at a certain proportion of data points despite the overall low energy storage parameter, indicating that some tight reservoirs in this area have certain storage space and flow capacity to a certain extent. In the area with a porosity of > 6%, most samples have high values of the energy storage parameter, and no data point is close to the horizontal axis, indicating that the tight reservoirs in this area have both high storage capacity and high seepage capacity.

(3) Ranking and evaluation of the reservoirs based on pore structure parameters

MICP can effectively reflect the configuration relationship of pore structure and the seepage capacity of tight reservoirs. MICP enjoys a low test cost and can reveal a wide range of pore sizes and yield accurate seepage parameters compared to rate-controlled mercury penetration, SEM, NMR, and CT scanning. Therefore, MICP is widely applied in tight reservoir evaluation [30, 31]. The main parameters used to evaluate reservoirs in mercury penetration experiments include the displacement pressure (P_d) and the

Table 1: Wettability measurement results of rocks in the Longfengshan sub-sag.

S.N.	Well No.	Depth (m)	Horizon	Wetting angle (°)	
				Water	Oil
1	Well Bei210	3944.85	Gas zone VI of Yingcheng Formation	51.27	Diffuse rapidly
2	Well Bei210	3945.33	Gas zone VI of Yingcheng Formation	52.55	Diffuse rapidly
3	Well Bei210	3946.45	Gas zone VI of Yingcheng Formation	32.88	Diffuse rapidly
4	Well Bei210	3948.07	Gas zone VI of Yingcheng Formation	51.47	Diffuse rapidly
5	Well Bei210	3949.5	Gas zone VI of Yingcheng Formation	31.97	Diffuse rapidly
6	Well Bei210	3951.15	Gas zone VI of Yingcheng Formation	56.9	Diffuse rapidly
7	Well Bei210	4127.9	Gas zone VI of Yingcheng Formation	50.35	Diffuse rapidly
8	Well Bei210	4129.65	Gas zone VI of Yingcheng Formation	26.33	Diffuse rapidly
9	Well Bei210	4129.95	Gas zone VI of Yingcheng Formation	45.85	Diffuse rapidly
10	Well Bei210	4130.35	Gas zone VI of Yingcheng Formation	31.74	Diffuse rapidly
11	Well Bei206	3234.89	Gas zone III of Yingcheng Formation	50.79	Spread out rapidly
12	Well Bei206	3243.6	Gas zone IV of Yingcheng Formation	44.72	Spread out rapidly
13	Well Bei206	3347.36	Gas zone IV of Yingcheng Formation	49.6	Spread out rapidly
14	Well Bei206	3409.82	Second member of Shahezi Formation	52.8	Spread out rapidly
15	Well Bei203	3317.87	Gas zone III of Yingcheng Formation	35.48	Spread out rapidly
16	Well Bei203	3318.15	Gas zone III of Yingcheng Formation	44.65	Spread out rapidly
17	Well Bei203	3615.5	Second member of Shahezi Formation	81.99	Spread out rapidly
18	Well Bei208	3261.45	Gas zone III of Yingcheng Formation	38.71	Spread out rapidly
19	Well Bei204	2368.78	Gas zone III of Yingcheng Formation	24.91	Spread out rapidly
20	Well Bei204	2389.4	Gas zone III of Yingcheng Formation	36.9	Spread out rapidly
21	Well Bei202	3112.75	Gas zone V of Yingcheng Formation	53.17	Spread out rapidly
22	Well Bei202	3128.6	Gas zone V of Yingcheng Formation	55.64	Spread out rapidly

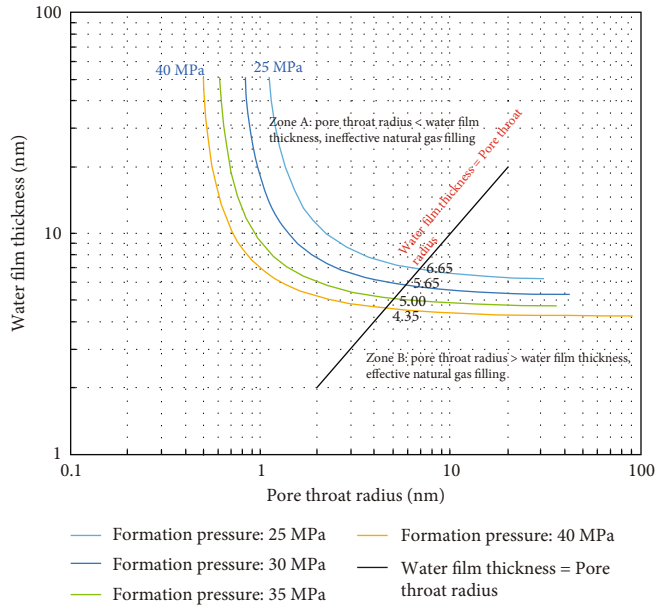

Figure 7: Relationship between the water film thickness and throat radius under different formation pressures of the Longfengshan area.

median pressure (P_{50}), which represent the minimum pressure required to displace water when oil and gas enter reservoirs and the median pressure represents the capillary pressure corresponding to the penetration saturation of 50%, respectively. Generally, a smaller displacement pressure corresponds to a lower median pressure, and both parameters can jointly reflect the tightness of rocks and the concentration of pore throat radius. A total of 34 MICP experiments were conducted in the Longfengshan area. Figure 5 shows the relationships of displacement pressure

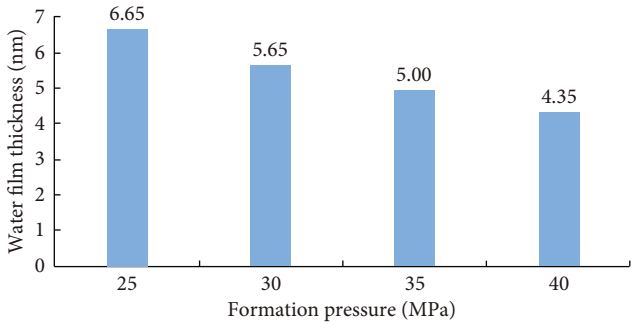

Figure 8: Histogram of the critical water film thickness under different formation pressures of the Longfengshan area.

and median pressure with the porosity of 34 samples. According to this figure, when the porosity is > 6%, both the displacement pressure and the median pressure are relatively low, and they are < 2 MPa and <20 MPa, respectively; when the porosity is 4%–6%, both the displacement pressure and the median pressure increase and are 2–6 MPa and 20–60 MPa, respectively; when porosity is < 4%, both displacement pressure and the median pressure sharply increase, and they are > 6 MPa and >60 MPa, respectively.

In addition, the structure coefficient and characteristic structure parameter in the MICP data are also important parameters used to characterize the homogeneity and fractal of cores. The structure coefficient represents the differences between real cores and the assumed model of parallel-tubular capillary bundles with the same length and cross-section area. Therefore, it can reflect the tortuosity degree of fluid seepage in pores. A high structure coefficient suggests strong pore tortuosity. The characteristic structure parameter can effectively characterize the relative sorting of pores. A high structure coefficient suggests good relative sorting of pores and a small difference between pore sizes. Figure 6 shows the relationships of the structure coefficient and the characteristic structure parameter with the porosity of samples from the study area. According to this figure, when the porosity is > 6%, the structure coefficient is high (>1), while the characteristic structure parameter is low (< 0.1); when the porosity is 4%–6%, the structure coefficient is 0.5–1 and the characteristic structure parameter is 0.1–0.2; when the porosity is < 4%, the structure coefficient is low (<0.5), while the characteristic structure parameter is high (>0.2). Therefore, the porosity boundaries corresponding to the structure coefficient and characteristic structure parameter are consistent with those corresponding to the displacement pressure and the median pressure.

Overall, the energy storage parameter and the pore structure parameters yielded consistent ranking results. Therefore, the porosity of 4% and 6% can be used as ranking boundaries of tight reservoirs, based on which the tight reservoirs can be divided into types I, II, and III.

I-type reservoirs have a porosity of > 6%, low displacement pressure, and high structure coefficients. The reservoirs of this type have high accumulation and seepage capacities.

II-type reservoirs have a porosity of 4%–6%, moderate displacement pressure, and moderate structure coefficients. The reservoirs of this type have moderate accumulation and seepage capacities due to their strong heterogeneity.

III-type reservoirs have a porosity of < 4%, high displacement pressure, and low structure coefficients. The reservoirs of this type have low accumulation and seepage capacities.

4. Discussion of the PPLL of Tight Sandstone Reservoirs

As long as oil and gas enter and fill tight reservoirs, tight oil and gas can be effectively developed using the horizontal well fracturing technology in theory. In other words, the PPLL of tight reservoirs is close to the lower limit of effective oil and gas filling [32]. Therefore, the water film thickness method is the most suitable to determine the PPLL of tight reservoirs due to its principle.

4.1. Determining the PPLL of Reservoirs Using Water Film Thickness Method

4.1.1. Rationality of Determining the Effectiveness of Oil and Gas Filling Using Water Film Thickness Method. Besides a high burial depth, the tight reservoirs in the Longfengshan area suffer low maturity, a high rock debris content, and strong compaction. Particles are cemented in the reservoirs by pores and compaction, resulting in primarily point-line contacts and line contacts between grains. Furthermore, the tight reservoirs tend to have strong hydrophilicity. In addition, multiple layers of water molecules occur between grain surface and rock matrix surface, and they are strongly bound water, weakly bound water, and then freely moving gravity water from inside to outside. Therefore, the minimum pore throat radius controlling oil and gas filling is the water film thickness under the critical state (the critical water film thickness), which is related to formation temperature and pressure.

5. Determining the Critical Water Film Thickness

Adsorbed water film results from the interactions between solid and liquid, and its thickness correlates with mineral composition and is related to formation temperature and pressure. Analyses reveal that, when gravity is not considered, the water film is subject to three pressures, namely the separation pressure (Pd) generated by its top approaching its bottom, the formation pressure (Pi) perpendicular to capillary walls, and the capillary pressure (Pc) in the opposite direction of formation pressure. Based on this and the method developed to determine the water film thickness by the authors in 2016 [33], the following equation can be obtained:

$$Pi = 2200/h^3 + 150/h^2 + 12/h + 2\sigma \cos\theta/r, \quad (2)$$

where

Pi: formation pressure, MPa

Table 2: Statistics of the lower limit of porosity in the Longfengshan area.

Well No.	Depth (m)	BET specific surface area ($m2 \cdot g^{-1}$)	Irreducible water saturation (%)	Water film thickness (nm)	Rock density ($g \cdot cm^{-3}$)	Lower limit of porosity (%)
Well Bei210	3944.85	1.82	55.71	3.99	2.50	3.48
Well Bei210	3946.45	1.20	53.78	3.99	2.51	2.32
Well Bei210	3949.5	1.87	70	3.98	2.62	3.75
Well Bei210	3951.15	1.53	56.9	3.98	2.50	2.92
Well Bei210	4127.9	1.22	50.35	3.95	2.55	2.37
Well Bei210	4129.65	0.58	26.33	3.95	2.63	1.16
Well Bei210	4129.95	1.35	45.85	3.95	2.63	2.71
Well Bei210	4130.35	0.91	31.74	3.95	2.62	1.81
Average lower limit of porosity (%)						2.56

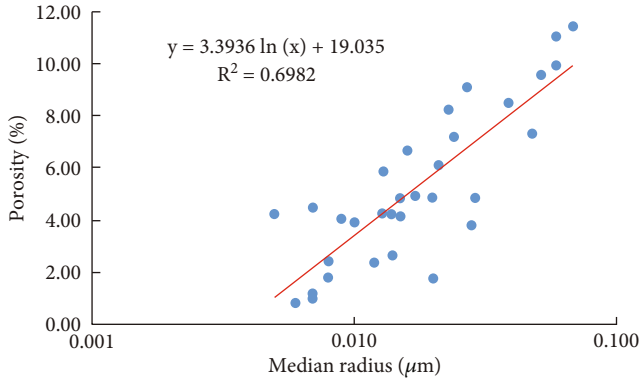

Figure 9: Cross-plot of the relationship between median radius and porosity.

h: water film thickness, μm
r: throat radius, μm
σ: gas-water interfacial tension, N/m
θ: wetting angle.

Among these five parameters, σ can be determined by referring to the gas-water interfacial tension previously measured, and θ can be obtained through wetting angle experiments on minerals. In this study, the wetting angles of 22 samples from the target horizon in the Longfengshan area were determined to be 45.49° on average using the contact angle goniometer LT/Y2009-005 and QB/T pendant drop method (Table 1).

After determining interfacial tension and wetting angle, the relationship between the water film thickness and throat radius under different formation pressures can be obtained using Equation (2), as shown in Figure 7. The curves in this figure represent the relationships under the formation pressures of 25Mpa, 30Mpa, 35Mpa, and 40Mpa. The critical state, at which the throat radius is equal to the water film thickness, corresponds to the intersections of the line $Y = X$ and the curves. As Figure 8 shows, the critical water film thickness gradually decreases as the formation pressure increases.

6. Converting the Critical Water Film Thickness into Porosity

As the PPLL of reservoirs, the nanoscale critical water film thickness is not practical in reservoir evaluation. By referring to the relationship between porosity and water film thickness in oil science, this study converted the critical water film thickness into the porosity, which is used as the lower limit of porosity. The conversion equation is as follows [34]:

$$\Phi = h \times A \times \rho / (7142 \times Swi), \quad (3)$$

where

Φ: the porosity of rocks, %
h: the film thickness of irreducible water, 0.10 nm
A: the specific surface area of rocks, m^2/g
S_{wi}: irreducible water saturation, %
ρ: the density of rock matrix, g/m^3.

The parameters such as irreducible water saturation and specific surface area were obtained through NMR and low-temperature nitrogen adsorption experiments. The lower limit of porosity of different samples can be obtained using these parameters and rock density. Table 2 shows the statistics of the lower limit of the porosity at the target horizon in Well Bei210 in the Longfengshan area. According to this table, the average lower limit of porosity of eight samples from the target horizon is 2.56%.

Table 3: Statistics of the lower limit of porosity obtained using the minimum flow pore throat radius method.

Well No.	Minimum flow pore throat radius (nm)	Lower limit of porosity (%)
Well Bei210	6.60	2.00
Well Bei202	7.75	2.54
Well Bei204	9.00	3.05
Well Bei208	6.50	1.94
Well Bei203	8.20	2.73
Well Bei206	6.10	1.73
Average		2.33

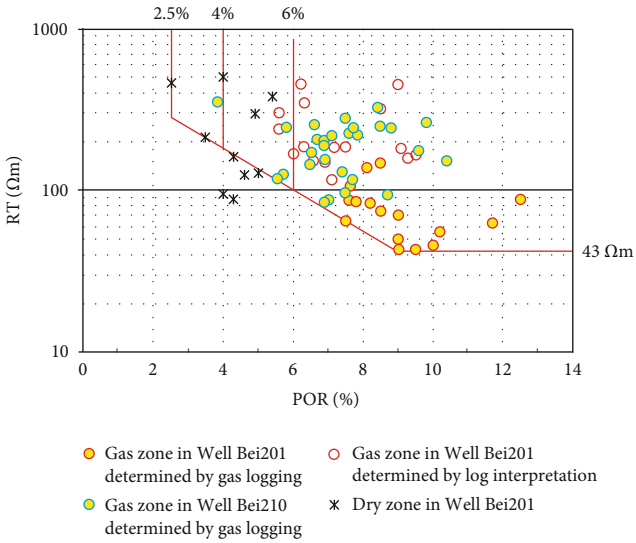

Figure 10: Scatter plot of results from gas logging and log interpretation of tight sandstone reservoirs.

6.1. Determining PPLL of Reservoirs Using the Minimum Flow Pore Throat Radius Method. The minimum flow pore throat radius method uses capillary pressure curves to calculate the minimum pore throat radius that allows fluids to flow. In this method, the contribution value of each throat radius to permeability is successively added. When the cumulative contribution value reaches 99.99%, the corresponding pore throat radius is the minimum flow pore throat radius [35, 36]. Figure 9 shows the relationship between the median pore throat radius and the porosity obtained using the MICP data of 32 tight sandstone samples from six wells in the study area. This figure shows a close linear relation (correlation coefficient: up to 0.69) between the median radius and the porosity.

Substituting the minimum flow pore throat radius of the six wells into the fitting formula between the median radius and the porosity yielded the lower limit of porosity (Table 3), which is 2.33% on average.

The water film thickness method and the minimum flowing pore throat radius method yielded approximate PPLL, which is 2.56% and 2.33%, respectively. Based on the comprehensive consideration of both methods, the PPLL of tight sandstone reservoirs in the Longfengshan area is finally determined to be 2.50%.

6.2. Case Analysis. The effects of the ranking and evaluation method proposed in this study in practical application were verified by the log interpretation of major exploration wells Bei210 and Bei201 in the Longfengshan area. Figure 10 shows the results of gas logging and log interpretation of tight sandstone reservoirs in the two wells (N =70). According to this figure, the physical properties of gas zones correspond closely to the ranking and evaluation results of the reservoirs obtained in this study. Specifically, high-quality gas zones in the tight sandstone generally have a porosity of greater than 6%; the reservoirs with a porosity of 4%–6% show the presence of both gas zones and dry zones; the reservoirs with a porosity of 2.5%–4% are dominated by dry zones, with a few of gas zones still developing. As verified using well logging and the porosity and permeability data, the ranking and evaluation standard of tight sandstone reservoirs proposed in this study is effective and can be applied to reservoir prediction.

7. Conclusions

(1) The lithology of the tight reservoirs in the Longfengshan area in the southern Songliao Basin mainly comprises medium-fine- and coarse-grained sandstones. Clastic grains in the reservoirs are dominated by rock debris. Moreover, the tight reservoirs have complex pore structures and show distinguishing characteristics of low porosity, low permeability, and poor pore throat connectivity

(2) The tight sandstone reservoirs in the Longfengshan area are divided into three types using the energy storage parameter and pore structure, and the corresponding porosity boundaries are 4% and 6%. Compared with traditional methods, the energy storage parameter has characteristics such as simple parameters and clear geological significance. It can comprehensively reflect the accumulation and seepage capacities of reservoirs and is applicable to tight sandstone reservoirs with strong heterogeneity

(3) The PPLL of tight sandstone reservoirs in the Longfengshan area was determined to be 2.50% using the water film thickness method and the minimum flow pore throat radius method. The water film thickness method, which comprehensively considers the geological factors including formation temperature, formation pressure, and the adsorption capacity of minerals, can accurately reflect the lower limit of oil and gas filling of oil reservoirs

(4) The ranks and PPLL of tight reservoirs can be accurately determined by comprehensively using the energy storage evaluation parameter, water film thickness, pore structure parameters, and minimum flow pore throat radius. This set of evaluation methods is innovative and can be widely applied

Data Availability

The basic research data for the research results come from PetroChina North China Petrochemical Company. The original contributions presented in the study are included in the article/supplementary material; further inquiries can be directed to the corresponding author.

Conflicts of Interest

The authors declare that the research was conducted in the absence of any commercial or financial relationships that could be construed as a potential conflict of interest.

Acknowledgments

This work was jointly funded by a project of the National Natural Science Foundation of China (41672125), the Shandong Provincial Natural Science Foundation (ZR2020MD0270), and China National Petroleum Corporation's "14th Five-Year" forward-looking basic major scientific and technological projects (2021DJ0203).

References

[1] G. Y. Zhu, L. J. Gu, J. Su et al., "Sedimentary association of alternated mudstones and tight sandstones in China's oil and gas bearing basins and its natural gas accumulation," *Journal of Asian Earth Sciences*, vol. 50, pp. 88–104, 2012.

[2] X. Fang, Z. Yang, W. P. Yan, X. G. Guo, Y. X. Wu, and J. T. Liu, "Classification evaluation criteria and exploration potential of tight oil resources in key basins of China," *Journal of Natural Gas Geoscience*, vol. 4, no. 6, pp. 309–319, 2019.

[3] Y. Li, J. H. Yang, Z. J. Pan, S. Z. Meng, K. Wang, and X. L. Niu, "Unconventional natural gas accumulations in stacked deposits: a discussion of upper paleozoic coal-bearing strata in the east margin of the Ordos basin, China," *Acta Geologica Sinica-English Edition*, vol. 93, no. 1, pp. 111–129, 2019.

[4] A. Li, W. L. Ding, and J. H. He, "Research on the types and characteristics of the tight sandstone gas reservoir forming mechanism," *Jilin Geology*, vol. 33, no. 2, pp. 8–12, 2014.

[5] H. Yang, "Formation conditions and exploration technology of large-scale tight sandstone gas reservoir in Sulige," *Acta Petrolei Sinica*, vol. 33, A supplement, pp. 27–36, 2012.

[6] Y. Li, X. D. Gao, S. Z. Meng et al., "Diagenetic sequences of continuously deposited tight sandstones in various environments: a case study from upper Paleozoic sandstones in the Linxing area, eastern Ordos basin, China," *AAPG Bulletin*, vol. 103, no. 11, pp. 2757–2783, 2019.

[7] N. N. Su, F. Song, L. W. Qiu, and W. Zhang, "Diagenetic evolution and densification mechanism of the Upper Paleozoic tight sandstones in the Ordos Basin, Northern China," *Journal of Asian Earth Sciences*, vol. 205, p. 104613, 2021.

[8] G. D. Liu, M. L. Sun, Z. Y. Zhao, X. B. Wang, and S. H. Wu, "Characteristics and accumulation mechanism of tight sandstone gas reservoirs in the Upper Paleozoic, northern Ordos Basin, China," *Petroleum Science: English edition*, vol. 10, no. 4, pp. 442–449, 2013.

[9] A. Jabir, A. Cerepi, C. Loisy, and J. Rubino, "Evaluation of reservoir systems in Paleozoic sedimentary formations of Ghadames and Jefarah basins," *Journal of African Earth Sciences*, vol. 183, no. 8, article 104324, 2021.

[10] P. Zhu, Y. X. Dong, M. Chen et al., "Quantitative evaluation of pore structure from mineralogical and diagenetic information extracted from well logs in tight sandstone reservoirs," *Journal of Natural Gas Science and Engineering*, vol. 80, p. 103376, 2020.

[11] H. X. Huang, W. Sun, M. L. Ji et al., "Effects of pore-throat structure on gas permeability in the tight sandstone reservoirs of the Upper Triassic Yanchang formation in the Western Ordos Basin, China," *Journal of Petroleum Science and Engineering*, vol. 162, pp. 602–616, 2018.

[12] Y. Gao, Z. Z. Wang, Y. Q. She, S. G. Lin, M. P. Lin, and C. L. Zhang, "Mineral characteristic of rocks and its impact on the reservoir quality of He 8 tight sandstone of Tianhuan area, Ordos Basin, China," *Journal of Natural Gas Geoscience*, vol. 4, no. 4, pp. 205–214, 2019.

[13] X. X. Kong, D. S. Xiao, S. Jiang, S. F. Lu, B. Sun, and J. M. Wang, "Application of the combination of high-pressure mercury injection and nuclear magnetic resonance to the classification and evaluation of tight sandstone reservoirs: a case study of the Linxing Block in the Ordos Basin," *Natural Gas Industry B*, vol. 7, no. 5, pp. 433–442, 2020.

[14] Q. H. Xiao, Z. Y. Wang, Z. M. Yang, Z. P. Xiang, Z. H. Liu, and W. Yang, "Novel method for determining the lower producing limits of pore-throat radius and permeability in tight oil reservoirs," *Energy Reports*, vol. 7, pp. 1651–1656, 2021.

[15] M. J. Liu, Z. Liu, Y. W. Wu, W. Q. Zhu, and P. Wang, "Differences in formation process of tight sandstone gas reservoirs in different substructures in Changling Fault Depression, Songliao Basin, NE China," *Petroleum Exploration & Development*, vol. 44, no. 2, pp. 257–264, 2017.

[16] Y. Q. Lu, Y. L. Jiang, W. Wang, J. F. Du, and J. D. Liu, "Coupling relationship between reservoir diagenesis and hydrocarbon accumulation in Lower Cretaceous Yingcheng Formation of Dongling, Changling fault depression, Songliao Basin, Northeast China," *China Geology*, vol. 3, no. 1, pp. 1–15, 2020.

[17] B. Liu, L. Jin, and C. Z. Hu, "Fractal characterization of silty beds/laminae and its implications for the prediction of shale oil reservoirs in Qingshankou Formation of northern Songliao Basin, Northeast China," *Fractals*, vol. 27, no. 1, pp. 1940009–1940012, 2019.

[18] B. Liu, S. L. He, L. D. Meng, X. F. Fu, L. Gong, and H. X. Wang, "Sealing mechanisms in volcanic faulted reservoirs in Xujiaweizi extension, Northern Songliao Basin, Northeastern China," *AAPG Bulletin*, vol. 105, no. 8, pp. 1721–1743, 2021.

[19] K. Q. Chen, J. L. Lu, X. Zhang, and H. L. Bi, "Characteristics and exploration potential of volcanic reservoirs in Changling fault depression in southern Songliao Basin," *Geological Bulletin*, vol. 30, no. Z1, pp. 228–234, 2011.

[20] J. Choma, J. Jagiello, and M. Jaroniec, "Assessing the contribution of micropores and mesopores from nitrogen adsorption on nanoporous carbons: Application to pore size analysis," *Carbon*, vol. 183, pp. 150–157, 2021.

[21] F. Zhang, Z. X. Jiang, W. Sun et al., "A multiscale comprehensive study on pore structure of tight sandstone reservoir realized by nuclear magnetic resonance, high pressure mercury injection and constant-rate mercury injection penetration test," *Marine and Petroleum Geology*, vol. 109, pp. 208–222, 2019.

[22] K. M. Askvik, S. HøIland, P. Fotland, T. Barth, and F. F. H. Grønn, "Calculation of wetting angles in crude oil/water/quartz systems," *Journal of Colloid & Interface Science*, vol. 287, no. 2, pp. 657–663, 2005.

[23] N. Gautier, D. R. Schmitt, and R. S. Kofman, "Pore systems in carbonate formations, Weyburn field, Saskatchewan, Canada: micro-tomography, helium porosimetry and mercury intrusion porosimetry characterization," *Journal of Petroleum Science and Engineering*, vol. 171, pp. 1496–1513, 2018.

[24] W. M. Wang, W. H. La, T. G. Fan, X. F. Xu, Y. N. Liu, and Q. X. Lv, "A comparative study on microscopic characteristics of volcanic reservoirs in the Carboniferous Kalagang and Haerjiawu formations in the Santanghu Basin, China," *Frontiers in Earth Science*, vol. 9, p. 728, 2021.

[25] B. Liu, L. H. Bai, M. Yan, X. D. Sun, X. F. Fu, and Y. F. Bai, "Microscopic and fractal characterization of organic matter within lacustrine shale reservoirs in the first member of

Cretaceous Qingshankou Formation, Songliao Basin, Northeast China," *Journal of Earth Science*, vol. 31, no. 6, pp. 1241–1250, 2020.

[26] C. N. Zou, R. K. Zhu, K. Y. Liu et al., "Tight gas sandstone reservoirs in China: characteristics and recognition criteria," *Journal of Petroleum Science and Engineering*, vol. 88–89, no. 2, pp. 82–91, 2012.

[27] R. L. Guo, Q. C. Xie, X. F. Qu et al., "Fractal characteristics of pore-throat structure and permeability estimation of tight sandstone reservoirs: a case study of Chang 7 of the Upper Triassic Yanchang Formation in Longdong area, Ordos Basin, China," *Journal of Petroleum Science and Engineering*, vol. 184, p. 106555, 2020.

[28] S. Yin, L. Dong, X. Yang, and R. Y. Wang, "Experimental investigation of the petrophysical properties, minerals, elements and pore structures in tight sandstones," *Journal of Natural Gas Science and Engineering*, vol. 76, p. 103189, 2020.

[29] A. Vafaie, I. R. Kivi, S. A. Moallemi, and B. Habibnia, "Permeability prediction in tight gas reservoirs based on pore structure characteristics: a case study from South Western Iran," *Resources*, vol. 1, pp. 9–17, 2021.

[30] C. Z. Li, G. D. Liu, Z. Cao, and M. L. Sun, "Oil charging pore throat threshold and accumulation effectiveness of tight sandstone reservoir using the physical simulation experiments combined with NMR," *Journal of Petroleum Science and Engineering*, vol. 2021, no. 6, article 109338, 2021.

[31] J. Lai and G. W. Wang, "Fractal analysis of tight gas sandstones using high-pressure mercury intrusion techniques," *Journal of Natural Gas Science & Engineering*, vol. 24, pp. 185–196, 2015.

[32] H. Pang, X. G. Ding, X. Q. Pang, and H. Geng, "Lower limits of petrophysical parameters allowing tight oil accumulation in the Lucaogou Formation, Jimusaer Depression, Junggar Basin, Western China," *Marine and Petroleum Geology*, vol. 101, pp. 428–439, 2018.

[33] W. M. Wang, S. X. Lu, W. C. Tian, and N. W. Zhou, "A new method to determine porosity and permeability cutoffs of tight oil reservoirs by using thickness of adsorption water film: a case study from the Damintun Sag, Liaohe oifield," *Oil and Gas Geology*, vol. 37, no. 1, pp. 135–140, 2016.

[34] X. Yang, D. Xiang, and Y. C. Yang, "Study of gas recovery and water film thickness in water drive for tight sandstone gas reservoir," *Journal of CHENGDU University of Technology*, vol. 26, no. 4, pp. 389–391, 1998.

[35] A. M. S. Lala and N. A. A. El-Sayed, "Controls of pore throat radius distribution on permeability," *Journal of Petroleum Science and Engineering*, vol. 157, pp. 941–950, 2017.

[36] D. Y. Zheng, X. Q. Pang, L. M. Zhou et al., "Critical conditions of tight oil charging and determination of the lower limits of petrophysical properties for effective tight reservoirs: a case study from the Fengcheng Formation in the Fengcheng area, Junggar Basin," *Journal of Petroleum Science and Engineering*, vol. 190, p. 107135, 2020.